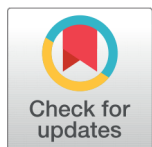


## RESEARCH ARTICLE

 OPEN ACCESS

Received: 21-02-2023

Accepted: 08-08-2023

Published: 19-09-2023

**Citation:** Agrawal K, Patel T, Thakur S, Patel K, Mittal S (2023) Spectral Investigations, DFT Studies, ADME Analysis, Molecular Docking of New Piperidine Derivatives with Potential Antimicrobial Activity. Indian Journal of Science and Technology 16(35): 2835-2844. <https://doi.org/10.17485/IJST/v16i35.389>

\* **Corresponding author.**[agrawalkhushbu007@gmail.com](mailto:agrawalkhushbu007@gmail.com)**Funding:** None**Competing Interests:** None

**Copyright:** © 2023 Agrawal et al. This is an open access article distributed under the terms of the [Creative Commons Attribution License](https://creativecommons.org/licenses/by/4.0/), which permits unrestricted use, distribution, and reproduction in any medium, provided the original author and source are credited.

Published By Indian Society for Education and Environment ([iSee](https://www.isee.org/))

**ISSN**

Print: 0974-6846

Electronic: 0974-5645

# Spectral Investigations, DFT Studies, ADME Analysis, Molecular Docking of New Piperidine Derivatives with Potential Antimicrobial Activity

Khushbu Agrawal<sup>1\*</sup>, Tarun Patel<sup>2</sup>, Shavi Thakur<sup>1</sup>, Kruti Patel<sup>1</sup>, Sumit Mittal<sup>3</sup>

<sup>1</sup> Department of Chemistry, Shree Maneklal M. Patel Institute of Sciences and Research, Sector 15/23, Kadi Sarva Vishwavidyalaya, Gandhinagar, 382023, Gujarat, India

<sup>2</sup> Department of Chemistry, Sir P T Science College, HNGU, Modasa

<sup>3</sup> School of Advanced Sciences and Languages (SASL), VIT Bhopal University, Kothri Kalan, Near Indore Road, Bhopal, 466114, Madhya Pradesh, India

## Abstract

**Objective:** To explore the possibility of obtaining effective and harmless antibacterial drugs by conventional synthesis of new piperidine analogs.

**Methods:** The target compound was carried out by cyclization reaction involving aromatic aldehydes and amine and further evaluated for their antimicrobiological assay using agar disc diffusion method. Computational investigation such as density functional theory (DFT) was carried out by B3LYP/6-31G (d,p) method to evaluate their electronic characteristics. Absorption, Distribution, Metabolism, and Excretion (ADME) properties were evaluated using the Swiss ADME server. The Antimicrobial activity was investigated using molecular docking and that molecule was prepared using MGL Tools 1.5.7. Auto Dock Vina 1.2.0. **Findings:** Among all the synthesized compounds 5a to 5h, compounds 5b and 5e showed good anti-bacterial properties against three pathogenic bacterial strains. *B. subtilis* is inhibited by compound 5b at a concentration of 26 mm. *B. subtilis* is inhibited by compound 5e at a concentration of 25 mm. Molecular Docking revealed that molecules 5b and 5e consistently showed a large binding affinity for all six target proteins, which was similar to that of the reference molecule, streptomycin. Drug-likeness predictions and the ADME analysis showed that most of the molecules do not violate any of the five Lipinski rule while some have only one or two violations, primarily because of high molecular weight. **Novelty:** In order to investigate the anti-bacterial impact of piperidine derivatives, a lot of work has been put into their synthesis and evaluation. These results might influence the creation and advancement of anti-microbial medication candidates that are more potent.

**Keywords:** Piperidine; Antimicrobial; SAR Study; Molecular Docking; ADME Study; DFT

## 1 Introduction

Heterocyclic compounds have been studied for centuries and are more important in Medicinal Chemistry and biology<sup>(1)</sup>. Synthesis of highly functionalized organic molecules is done using multicomponent reactions. Researchers have thoroughly exploited these structural features of heterocycles over the last three decades<sup>(2)</sup>.

Piperidine-4-ones and its derivative is a nitrogen-containing saturated six-membered heterocyclic ring<sup>(3)</sup>. It's found in a wide range of active synthetic pharmaceuticals. Piperidine derivatives are a intriguing class of N-heterocycles observed in medicinal medicines and antiproliferative, antitubercular, and antioxidant, chiral molecules that have significant biological activity, such as antihypertensive, antibacterial, anticonvulsant, antimalarial, anti-inflammatory<sup>(4-6)</sup>.

In 2023, D.P. Ganesha and his team investigate Piperidine-4-one derivative as antimicrobial agents. Derivatives of 2,6-disubstituted piperidin-4-ones were prepared by R. Srikanth and co researchers,2016. After that prepared derivatives were investigated for microbiological activity. In 2023, The Plastoquinone analogues synthesized by Mahmut Yildiz and team were composed of a modified quinone ring, connected to a piperidine moiety. The piperidine moiety was designed to enhance the overall efficacy of the analogues, and to improve their potential to act as antimicrobial agents<sup>(7,8)</sup>. In 2022, Abeer Hussein Ali conducted a groundbreaking investigation into the properties of a new Schiff base derivative of piperidine. The derivative was tested for its biological activity against a range of gram-positive and gram-negative bacteria. The results of this research indicated that the derivative had a promising potential for medical applications, particularly in the treatment of bacterial infections. Further research will be needed to determine the full range of potential benefits. In the meantime, Ali's research provides a promising foundation for further exploration<sup>(9)</sup>. In this present study, We Synthesized and investigate various novel piperidine-4-one derivatives with potentially enhanced features because piperidine has been successful as a drug precursor. Motivated by the literature we synthesized structurally different piperidine-4-one derivative and screened them for anti-bacterial activity against *B. subtilis*, *S. aureus* and *E. coli*, *P. aeruginosa* bacterial strains. Additionally, DFT study is also performed in order to optimize geometry of the molecules. To understand to relationship between ligand-protein Molecular docking is performed against six selected proteins, namely *S. aureus* Sortase-A (PDB 5D: **1T2P**), *B. subtilis* aminoglycoside 6-adenyltransferase (PDB 5D: **2PBE**), *S. aureus* Dihydrofolate reductase (PDB 5D: **2W9S**), *S. aureus* Undecaprenyl diphosphate synthase (PDB 5D: **4H8E**), *S. aureus* Staph Gyrase B (PDB 5D: **4URO**), *E. coli* gyrase B (PDB 5D: **6F86**). In order to investigate the pharmacokinetic profile of the compounds synthesized in the current study, in silico ADME calculations have been utilized. This involves the use of computational tools to predict the absorption, distribution, metabolism, excretion (ADME) of the compounds. These calculations can provide an efficient and cost-effective method of assessing the pharmacokinetics of the compounds. By making use of these calculations, the overall safety and efficacy of the compounds can be determined even before they are tested in the laboratory. This can help to streamline the drug development process and significantly reduce the time and cost associated with it. Here, anti-microbial activity is described by structure activity relationship of synthesized piperidine-4-one derivative

## 2 Methodology

AR grade reagents and solvents were used throughout the experiment. Thin-layer chromatography (TLC) with silica gel G plates revealed that the reactions progressed using solvent systems of chloroform: ethyl acetate: chloroform (3: 2 v/v) and chloroform: ethyl acetate: chloroform (5:5 v/v). To characterize the <sup>1</sup>H NMR and mass spectra of the derivatives, different instruments were used, such as the Bruker 400 MHz, LC-MS spectrometer. The data obtained from the instruments was used to analyze the reaction products and to determine the purity of the derivatives. The LC-MS spectrometer was used to measure the molecular weights of the derivatives, which provided further evidence of the successful synthesis of the desired products. The <sup>1</sup>H NMR spectra were used to determine the precise structure of the derivatives and to provide a more complete understanding of the reaction.

### 2.1 General procedure for synthesizing of (E) -1-(4-(piperidin-4-ylamino phenyl) -3-(m-tolyl) prop-2-en-1-one derivatives

In two necked RBFs, a mixture of 0.1 mol 4-chloropiperidine and 0.05 mol 1-(4-aminophenyl) ethenone was added, then refluxed for 10–12 hours with constant stirring. 1-(4-(piperidine-4-ylamino) phenyl) ethenone is yielded after cooling and drying process of reaction mixture<sup>(10)</sup>, 0.03 mol potassium hydroxide, 0.01 mol aldehyde and yielded product were refluxed in the presence of ethanol as solvent<sup>(11)</sup> The process of making piperidine derivatives began by cooling and drying the reaction. The resultant precipitate firstly filtered then washed and dried. In order to purify the product, ethanol was used in combination with a recrystallization technique. According to existing literature data on piperidine scaffolds and related to same piperidine derivatives, presently we discovered (E) -1-(4-(piperidine-4-ylamino) phenyl) - 3-(m-tolyl) prop- 2- en- 1-one derivatives and

related variety of derivatives. The Figure 1 is showing the synthetic route for present derivative.

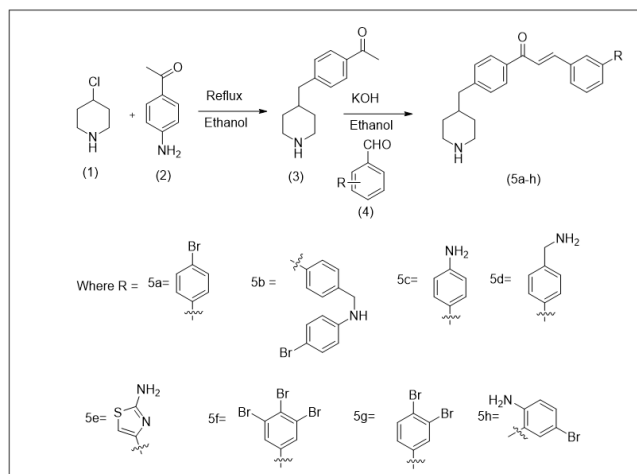


Fig 1. Synthetic route of (E)-1-(4-(piperidin-4-ylamino)phenyl)-3-(m-tolyl)prop-2-en-1-one

## 2.2 In-vitro antimicrobial activity

The antibacterial potential of the synthesized analogues (5a-5h) was examined by Agar disc diffusion method<sup>(12,13)</sup>. The disc diffusion method was utilized to test the antimicrobial efficiency of synthesized compounds. Gram-positive (*B. subtilis* and *S. aureus*) and two Gram-negative (*E. coli* and *P. aeruginosa*) bacterial strains were chosen and seeded onto a previously sterilized nutrient agar. As a control sample, DMSO-containing discs were used. In each of the Petri plates, prepare sterile (Hi-Media) discs of 10 mm in diameter, after that add 50  $\mu$ L of all synthetic mixture (1 mg/mL i.e. 50 g/disc) and incubate at 37<sup>o</sup>C for 24 hours. The results of the activity tables showed that the parent molecule had no antibacterial potential against any of the Gram-positive/Gram-negative bacteria tested after 24 hours of incubation at 25  $\pm$  2 <sup>o</sup>C. The size of the resulting zone of inhibition was then measured. It was observed that the zone of inhibition was not present in the control, indicating that the parent molecule had no antibacterial activity. This result was consistent with the activity table results<sup>(14)</sup>.

## 2.3 Media preparation

Antimicrobial testing against four bacteria, *B. subtilis*, *S. aureus* and *E. coli*, *P. aeruginosa* was performed using disc diffusion method. The biological assay was performed on Muller-Hinton agar (MHA). To prepare the medium, in 100 mL distilled water 3.8 gm of MHA was dissolved. The medium is gently heated with frequent agitation to achieve a homogeneous solution.

Once the medium was boiled for one min., it was autoclaved to maintain temp. of 121 <sup>o</sup>C for 15 min. After this, it was cooled to 25 <sup>o</sup>C. The medium's pH was kept constant at 7.1. This process ensured that the medium was of the highest quality and free from contamination.

## 2.4 Computational Study

The starting structural models for all (E)-1-(4-(piperidin-4-ylamino)phenyl)-3-(m-tolyl)prop-2-en-1-one derivative molecules were constructed using Gauss View 5 software<sup>(15)</sup>. All the molecules were next subjected to geometry optimization in the gas phase at the B3LYP/6-31G (d, p) level of theory as implemented in Gaussian 09 quantum chemistry package<sup>(16)</sup>. No symmetry constraints were imposed during the optimization. The molecular orbital was visualized and the associated energies were computed using Gauss View 5. Various other electronic properties, such as electronegativity, global hardness, global softness, and electrophilicity, were also computed for the optimized geometry using Gauss View 5.

The optimized geometry for each molecule was used to perform molecular docking against six target proteins, namely Staphylococcus aureus Sortase-A (PDB 5D: 1T2P), Bacillus subtilis aminoglycoside 6-adenyltransferase (PDB 5D: 2PBE), Staphylococcus aureus Dihydrofolate reductase (PDB 5D: 2W9S), Staphylococcus aureus Undecaprenyl diphosphate synthase (PDB 5D: 4H8E), Staphylococcus aureus Staph Gyrase B (PDB 5D: 4URO), *E. coli* gyrase B (PDB 5D: 6F86)<sup>(17–20)</sup>. The PDB

file of the target proteins were extracted from the RCSB protein data bank. Next, each target protein was prepared for docking by removing any existing ligand and water molecules, followed by charge assignment using MGL Tools 1.5.7.<sup>(21)</sup> Next, the grid box corresponding to the whole protein was defined for each target. Each derivative molecule was then prepared for docking using MGL Tools 1.5.7. Auto Dock Vina 1.2.0<sup>(22)</sup> was then used for docking the ligand molecules against the target proteins. For each molecule, 10 conformations were generated and the most favorable conformation, based on the binding affinity, was selected for further structural analysis. The non-covalent interactions between the protein and docked ligand were analyzed and visualized using Lig Plot software<sup>(23)</sup>. The procedure was followed for docking the reference molecule, streptomycin, against the target proteins.

Next, we performed the Absorption, Distribution, Metabolism, and Excretion (ADME) analysis for each derivatized molecule using the Swiss ADME server<sup>(24)</sup>. Various relevant parameters, such as the Lipinski's rule of five violations, number of hydrogen donors, hydrogen acceptors, rotatable bonds, total polar surface area, skin permeability (Log Kp), gastro-intestinal absorption (GI), blood brain barrier (BBB), inhibition of cytochromes P450 isoforms (CYP1A2, CYP2C19, CYP2C9, CYP2D6) were extracted from the calculation.

### 3 Results and Discussion

#### 3.1 Antibacterial Activity

Compounds 5a–h was tested for antibacterial activity and compared to streptomycin, a standard drug. When compared to other compounds, compounds 5b and 5e showed good antibacterial properties against three pathogenic bacterial strains. *B. subtilis* is inhibited by Compound 5b at a concentration of 26 mm. *B. subtilis* is inhibited by compound 5e at a concentration of 25 mm. The antibacterial activity of compounds 5g and 5h against four pathogenic bacterial strains was moderate. Compounds 5a and 5c showed weak antibacterial activity against *S. aureus* and *P. aeruginosa*. All the statistical data of biological activity is shown in Table 1.

**Table 1.** In Vitro antibacterial activities of compounds 5a–h

Zone of inhibition in diameter (mm) and MIC( $\mu\text{g/ml}$ )								
Compound	<i>B. subtilis</i>		<i>S. aureus</i>		<i>P. aeruginosa</i>		<i>E. coli</i>	
	Mm	MIC ( $\mu\text{g/ml}$ )	mm	MIC ( $\mu\text{g/ml}$ )	mm	MIC ( $\mu\text{g/ml}$ )	mm	MIC ( $\mu\text{g/ml}$ )
<b>5a</b>	19	09	10	08	11	08	11	09
<b>5b</b>	26	06	15	06	24	06	16	06
<b>5c</b>	22	07	12	09	19	05	12	06
<b>5d</b>	22	07	12	09	13	09	16	04
<b>5e</b>	25	06	14	08	23	05	17	05
<b>5f</b>	20	08	13	07	19	06	14	04
<b>5g</b>	18	07	10	05	10	08	11	09
<b>5h</b>	21	06	11	06	12	07	12	08
<b>Streptomycin</b>	26	06	18	06	25	05	20	05

#### 3.2 DFT Calculations

All the derivative complexes were optimized using the DFT methods at the B3LYP/6-31G(d, p) level of theory. The optimized geometries are shown in Figure 2 and the various electronic properties are presented in Table 2. The negative values of  $E_{HOMO}$  and  $E_{LUMO}$  for all derivative molecules indicate their stability. Further, Frontier Molecular Orbital analysis illustrates that the lowest occupied molecular orbital (LUMO) orbital is localized on the p orbitals of the phenyl ring and the linked ethylenic unit, (-CH=CH-) molecule in all complex molecules (Figure 3). However, the highest occupied molecular orbital (HOMO) orbital is either localized on the (E)-1-(4-(piperidin-4-ylamino) phenyl)- region (5a, 5d, 5e, 5f, 5g) or the substituted domain (5b, 5c, 5h). Moreover, the energy gap ( $E_{HOMO}-E_{LUMO}$ ), which is an important parameter to assess the thermal stability and the chem5cal reactivity of a molecule, was found to be negative for all the molecules suggesting high chemical reactivity for all the molecules and in the following order: 5d > 5e > 5a > 5g > 5b > 5h > 5f > 5c. We also computed additional electronic and structural parameters, such as electronegativity ( $\chi$ ), global hardness ( $\eta$ ), global softness ( $\sigma$ ), and global electrophilicity index

( $\omega$ ), to ascertain the biological activity of the derivative molecules (Table 2). The large  $\chi$  and  $\omega$  for all compounds indicate their excellent bioactivity. Interestingly, an excellent correlation ( $R^2 = 0.95$ ) was observed between the computed dipole moment of the molecules with their experimentally measured melting point, providing a rationale for their relative stability.

**Table 2.** The calculated  $E_{HOMO}$ ,  $E_{LUMO}$  (eV),  $E_{HOMO} - E_{LUMO}$  (DE, eV), electronegativity ( $\chi$ ), chemical potential ( $\mu$ ), global hardness ( $\eta$ ), global softness ( $\sigma$ ), and global electrophilicity index ( $\omega$ ) for derivative molecules as calculated at the B3LYP/6-31G(d,p) level of theory

	$E_{HOMO}$ (eV)	$E_{LUMO}$ (eV)	$E_{HOMO} - E_{LUMO}$ (eV)	$\chi$ (eV)	$\eta$ (eV)	$\Sigma$ (eV <sup>-1</sup> )	$\omega$ (eV)	Dipole Moment (D)
<b>5a</b>	-0.2009	-0.0716	-0.1293	0.1362	0.0646	15.4691	0.1436	7.6787
<b>5b</b>	-0.1961	-0.0688	-0.1274	0.1325	0.0637	15.7048	0.1378	7.8547
<b>5c</b>	-0.1872	-0.0629	-0.1243	0.1251	0.0622	16.0901	0.1258	3.5878
<b>5d</b>	-0.1976	-0.0658	-0.1318	0.1317	0.0659	15.1803	0.1317	4.2144
<b>5e</b>	-0.1964	-0.0647	-0.1317	0.1306	0.0658	15.1872	0.1295	3.4456
<b>5f</b>	-0.2031	-0.0763	-0.1268	0.1397	0.0634	15.7754	0.1540	4.0168
<b>5g</b>	-0.2019	-0.0737	-0.1281	0.1378	0.0641	15.6091	0.1482	8.8633
<b>5h</b>	-0.1961	-0.0691	-0.1271	0.1326	0.0635	15.7406	0.1384	8.0535

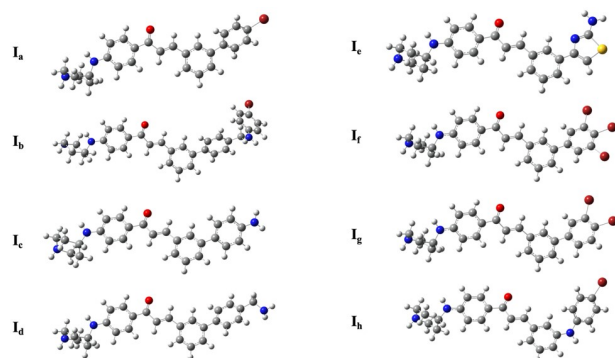


**Fig 2.** The geometry of derivative molecules at the B3LYP/6-31G(d,p) level of theory

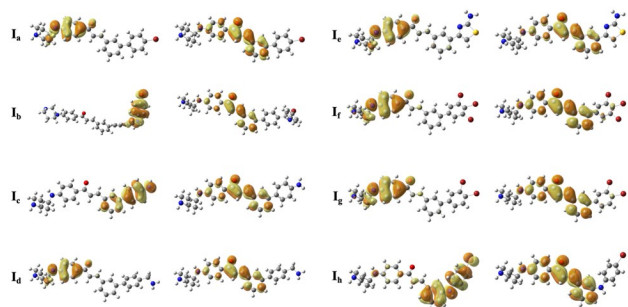


**Fig 3.** The HOMO and LUMO orbitals for the derivative molecules as calculated at the B3LYP/6-31G(d,p) level of theory

### 3.3 Docking Calculations

The derivative molecules were next subjected to molecular docking to assess their antibacterial potential. To this end, we used the geometry-optimized derivative molecules to perform molecular docking against various target molecules. Here, six target proteins were selected, representing different biologically important processes of the bacteria. The relative stability of the target

protein-ligand complex was determined by their binding affinities. Molecules 5b and 5e consistently showed a large binding affinity for all six target proteins, which was similar to that of the reference molecule, streptomycin (Figure 4, Table 3) The highest binding affinities were observed against 2W9S, 4H8E, and 1T2P proteins (Figure 5). Further analysis of the protein-ligand complex revealed a higher number of interactions in the case of 5b and 5e (Figure 6).

**Table 3.** Calculated docking affinities (in kcal/mol) of the derivative molecules and streptomycin against the six target proteins

	Docking Score (kcal/mol)					
	1T2P	2PBE	2W9S	4H8E	4URO	6F86
5a	-9.8	-8.6	-10.6	-10.2	-7.4	-7.4
5b	-10.1	-8.9	-11.1	-10.5	-7.8	-7.8
5c	-9.3	-8.5	-10.4	-9.9	-7.4	-8.1
5d	-9.1	-8.0	-10.4	-8.9	-7.5	-7.5
5e	-10	-8.8	-11.1	-11.1	-7.9	-7.5
5f	-8.9	-8.3	-10.4	-9.0	-7.5	-8.0
5g	-8.9	-8.1	-10.7	-10.3	-7.6	-7.5
5h	-8.9	-7.8	-10.5	-9.9	-7.4	-7.4
Streptomycin	-10.3	-10.3	-11.5	-12.2	-9.8	-10.7

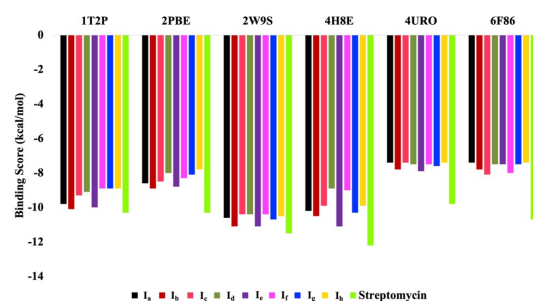


**Fig 4.** Comparison of the calculated docking affinities (in kcal/mol) of the derivative molecules and streptomycin against the six target proteins

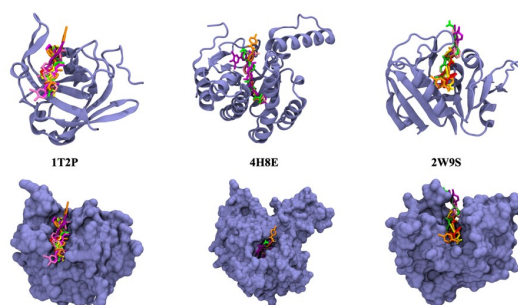


**Fig 5.** Overlay of the protein-derivative molecule complexes as obtained from their docking with 11T2P, 4H8E and 2W9S target proteins. The docked poses were chosen based on their bindingaffinities and geometrically similarities. The space-filled model of the complexes are also shown

### 3.4 ADME Calculations

Drug-likeness predictions and the ADME analysis showed that most of the molecules do not violate any of the five Lipinski rule (5c, 5d, 5e, and 5h) while some have only one or two violations, primarily because of the high molecular weight (Table 4). Therefore, these molecules have good potential as orally active drugs. The TPSA value, closely related to the bioavailability, for the molecules were observed in the range of 41 Å<sup>2</sup> to 108 Å<sup>2</sup>, which is well below the limit of 140 Å<sup>2</sup>. Similarly, the number of rotatable bonds (NRB) for all molecules is less than the limit of 10, suggesting that the molecules are conformationally stable.

Moreover, the low skin permeability value (Log K<sub>p</sub>) for all molecules indicates a low level of skin permeation (Table 5). All derivative molecules, except 5f, also showed a high level of gastrointestinal (GI) absorption. Similarly, all molecules, barring 5b and 5f, showed blood-brain barrier (BBB) permeation. The inhibition of cytochromes P450 isoforms (CYP1A2, CYP2C19, CYP2C9, CYP2D6) by the molecule is also essential in its toxic or side effects. Swiss ADME predictions showed that only molecule 5e has an inhibition propensity against all these isoforms. Other molecules, including 5b, which showed the highest binding affinity, fail to inhibit one or more of these isoforms. Considering all the ADME predictions as well as the binding affinities, molecule 5e appears as the most effective lead as an anti-bacterial agent. Intermolecular interactions between the derivation molecules and the *S. aureus* Dihydrofolate reductase (PDB 5D: 2W9S) target protein are shown in Figure 6.

**Table 4.** Drug-likeness predictions for the derivative molecules as computed using Swiss ADME. The number of rotatable bonds (NRB), number of hydrogen donors (NHD), number of hydrogen acceptors (NHA), total polar surface area (TPSA), LogP value and Lipinski's rule of five violation (LV) are reported

	NRB	NHA	NHD	TPSA (Å <sup>2</sup> )	LogP	LV
5a	6	2	2	41.13	5.26	1
5b	9	2	3	53.16	6.32	2
5c	6	2	3	67.18	4.11	0
5d	7	3	3	67.15	4.03	0
5e	6	3	3	108.28	3.64	0
5f	6	2	2	41.13	6.44	2
5g	6	2	2	41.13	5.84	2
5h	7	2	3	53.16	5.03	0

**Table 5.** Absorption, Distribution, Metabolism, and Excretion (ADME) analysis for the derivative molecules as computed using Swiss ADME. Skin permeability (Log K<sub>p</sub>), gastro-intestinal absorption (GI), blood brain barrier (BBB), and inhibition of cytochrome-P isoforms are reported

	Log K <sub>p</sub>	GI Absorption	BBB Absorption	Inhibitor Interaction			
				CYP1A2	CYP2C19	CYP2C9	CYP2D6
5a	-4.77	High	Yes	Yes	Yes	No	Yes
5b	-4.37	High	No	Yes	No	No	Yes
5c	-5.36	High	Yes	Yes	Yes	No	Yes
5d	-5.77	High	Yes	Yes	Yes	No	Yes
5e	-5.83	High	Yes	Yes	Yes	Yes	Yes
5f	-4.75	Low	No	No	Yes	No	Yes
5g	-4.76	High	No	No	Yes	No	Yes
5h	-4.92	High	Yes	Yes	Yes	No	Yes

### 3.5 Structure-Activity Relationship

Compounds 5g and 5h appear to be moderately active based on the results. As shown in Table 1, the Anti-microbial activity of synthesized compounds was compared to that of standard drugs. For the compounds 5a–h, an initial structure-activity relationship can be drawn. Different electron withdrawing and electron donating groups attached to aromatic rings as substituents were linked to the phenyl ring linked to the (-CH=CH-) group in the current study. The inhibition values of all the compounds exhibited a varied range (10–26 mm and 10–18 mm) of antibacterial activities against all the tested microbial strains, according to a thorough examination of the Antimicrobial efficacy. Enhanced activity is produced due to

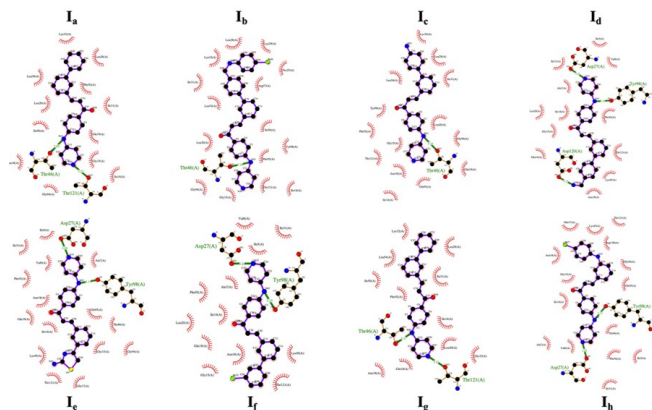


**Fig 6.** Intermolecular interactions between the derivative molecules and *Staphylococcus aureus* Dihydrofolate reductase (PDB 5D: 2W9S) target protein. The hydrogen bond interactions are highlighted

the presence of a heterocyclic ring in 5e. The derivative 5b showed increased anti-microbial activity due to the presence of the secondary amine attached to the benzyl ring. The rest of the derivatives showed moderate potency against anti-microbial agents. The Antimicrobial activity is influenced by the nature of the linkage (substituent on an aromatic ring), according to the SAR correlation studies.

### 3.6 Spectroscopic Characterization

In the present study, we have synthesized (5a-5h) derivatives of (E)-1-(4-(piperidin-4-ylamino) phenyl)-3-(m-tolyl) prop-2-en-1-one as outlined in Scheme 1. The structures of the components were reinforced by the  $^1\text{H}$  NMR, and mass spectral data (Supplementary File). The spectral data is as follows:

#### 3.6.1 Compound (5a) : (E)-3-(4'-bromo-[1,1'-biphenyl]-3-yl)-1-(4-(piperidin-4-ylamino) phenyl) prop-2-en-1-one

$^1\text{H}$  NMR in  $\text{CDCl}_3$  (400 MHz):  $\delta$  0.91-1.94 (4H, m,  $J = 13.1$ , -H of piperidine ring), 2.91- 3.04 (4H, m,  $J = 9.3$ , -H of piperidine ring), 3.78 (1H, t,  $J = 10.2$ , -H of piperidine ring), 6.66 (1H, d,  $J = 15.7$ , =CH-CO), 6.93 (2H, d,  $J = 8.5$ , at C-2, C-6 position of ArH), 7.19-7.37 (4H, d,  $J = 8.0$ , ArH), 7.40 (1H, d,  $J = 15.7$ , Ar-CH=), 7.38 (2H, d,  $J = 8.9$ , at C-2, C-6 position of Ar-Br), 7.42 (2H, d,  $J = 8.9$ , at C-3, C-5 position of Ar-Br), 7.69 (2H, d,  $J = 8.5$ , 1.8, at C-3, C-5 position of Ar-C=O).

#### 3.6.2 Compound (5b) : (E)-3-(4'-((4-bromophenyl amino) methyl) -[1,1'-biphenyl]-3-yl)-1-(4-(piperidin-4-ylamino) phenyl) prop-2-en-1-one

$^1\text{H}$  NMR in  $\text{CDCl}_3$  (400 MHz):  $\delta$  0.85-1.86 (4H, m,  $J = 13.1$ , -H of piperidine ring), 2.07-2.92 (4H, m,  $J = 9.3$ , -H of piperidine ring), 3.79 (1H, t,  $J = 10.2$ , -H of piperidine ring), 4.50 (2H, s, -CH<sub>2</sub> of R), 6.54 (2H, d,  $J = 8.3$ , at C-2, C-6 position of R), 6.68 (1H, d,  $J = 15.7$ , =CH-CO), 6.71 (2H, d,  $J = 8.5$ , at C-2, C-6 position of ArH), 7.16 (2H, d,  $J = 8.3$ , at C-3, C-5 position of R), 7.28-7.38 (3H, d,  $J = 8.0$ , ArH), 7.50 (2H, d,  $J = 8.4$ , at C-3, C-5 position of R), 7.52 (1H, d,  $J = 15.7$ , Ar-CH=), 7.61 (2H, d,  $J = 8.5$ , at C-3, C-5 position of ArH), 7.62 (2H, d,  $J = 8.4$ , at C-2, C-6 position of R), 7.90 (1H, d,  $J = 1.9$ , ArH).

#### 3.6.3 Compound (5c) : (E)-3-(4'-amino-[1,1'-biphenyl]-3-yl)-1-(4-(piperidin-4-ylamino) phenyl) prop-2-en-1-one

$^1\text{H}$  NMR in  $\text{CDCl}_3$  (400 MHz):  $\delta$  1.58-1.74 (4H, m,  $J = 13.1$ , -H of piperidine ring), 2.50-3.00 (4H, m,  $J = 9.3$ , -H of piperidine ring), 3.69 (1H, t,  $J = 10.2$ , -H of piperidine ring), 6.69 (1H, d,  $J = 15.7$ , =CH-CO), 6.90 (2H, d,  $J = 8.5$ , at C-2, C-6 position of ArH), 7.11 (2H, d,  $J = 8.9$ , at C-3, C-5 position of Ar-NH<sub>2</sub>), 7.35 (2H, d,  $J = 8.9$ , at C-3, C-5 position of Ar-NH<sub>2</sub>), 7.35-7.58 (4H, d,  $J = 8.0$ , ArH), 7.53 (1H, d,  $J = 15.7$ , Ar-CH=), 7.68 (2H, d,  $J = 8.5$ , at C-3, C-5 position of Ar-C=O).

#### 3.6.4 Compound (5d) : (E)-3-(4'-(aminomethyl) -[1,1'-biphenyl]-3-yl)-1-(4-(piperidin-4-ylamino) phenyl) prop-2-en-1-one

$^1\text{H}$  NMR in  $\text{CDCl}_3$  (400 MHz):  $\delta$  1.30-1.96 (4H, m,  $J = 13.1$ , -H of piperidine ring), 2.15- 3.55 (4H, m,  $J = 9.3$ , -H of piperidine ring), 3.78 (1H, t,  $J = 10.2$ , -H of piperidine ring), 4.02 (2H, s, -CH<sub>2</sub> of R), 6.78 (1H, d,  $J = 15.7$ , =CH-CO), 6.92 (2H, d,  $J = 8.5$ ,

at C-2, C-6 position of ArH), 7.05 (1H, d, J = 15.7, Ar-CH=), 7.24 (2H, d, J = 8.9, at C-3, C-5 position of Ar of R), 7.32 (2H, d, J = 8.5, 1.8, at C-3, C-5 position of Ar-C=O), 7.41-7.67 (4H, d, J = 8.0, ArH), 7.69 (2H, d, J = 8.9, at C-2, C-6 position of Ar of R).

### 3.6.5 Compound (5e) : (E)-3-(3-(2-aminothiazol-4-yl) phenyl) -1-(4-(piperidin-4-ylamino) phenyl) prop-2-en-1-one

<sup>1</sup>H NMR in CDCl<sub>3</sub> (400 MHz): δ 1.62-1.94 (4H, m, J = 13.1, -H of piperidine ring), 2.40- 3.06 (4H, m, J = 9.3, -H of piperidine ring), 3.79 (1H, t, J = 10.2, -H of piperidine ring), 6.65 (1H, d, J = 15.7, =CH-CO), 6.94 (2H, d, J = 8.5, 1.1, at C-2, C-6 position of ArH), 7.20 (1H, s, H attached to R), 7.40 (1H, d, J = 8.0, ArH), 7.59 (1H, d, J = 15.7, Ar-CH=), 7.40-7.68 (2H, d, J = 8.0, ArH), 7.68 (2H, d, J = 8.5, at C-3, C-5 position of Ar-C=O), 7.88 (1H, d, J = 8.0, ArH).

### 3.6.6 Compound (5f) : (E) -1-(4-(piperidin-4-ylamino) phenyl) -3-(3',4',5'-tribromo-[1,1'-biphenyl]-3-yl) prop-2-en-1-one

<sup>1</sup>H NMR in CDCl<sub>3</sub> (400 MHz): δ 1.45-1.67 (4H, m, J = 13.1, -H of piperidine ring), 2.31- 2.99 (4H, m, J = 9.3, -H of piperidine ring), 3.70 (1H, t, J = 10.2, -H of piperidine ring), 6.56 (1H, d, J = 15.7, =CH-CO), 6.84 (2H, d, J = 8.5, at C-2, C-6 position of ArH), 7.50 (1H, d, J = 7.9, ArH), 7.51-7.57 (2H, dd, J = 7.8, ArH), 7.59 (1H, d, J = 15.7, Ar-CH=), 7.68 (2H, d, J = 8.5, at C-3, C-5 position of Ar-C=O), 7.80 (2H, d, J = 1.8 Hz), 7.83 (1H, t, J = 1.9, ArH).

### 3.6.7 Compound(5g) : (E)-3-(3',4'-dibromo-[1,1'-biphenyl]-3-yl) -1-(4-(piperidin-4-ylamino phenyl) prop-2-en-1-one

<sup>1</sup>H NMR in CDCl<sub>3</sub> (400 MHz): δ 1.29-1.64 (4H, m, 1.63 (d, J = 13.1, -H of piperidine ring), 2.25- 2.96 (4H, m, J = 9.3, -H of piperidine ring), 3.94(1H, t, J = 10.2, -H of piperidine ring), 6.67 (1H, d, J = 15.7, =CH-CO), 6.72 (2H, d, J = 8.5, at C-2, C-6 position of ArH), 7.19 (1H, d, J = 8.8, ArH of R), 7.23 (2H, d, J = 7.9, ArH), 7.30 (1H, d, J = 15.7, Ar-CH=), 7.37 (1H, d, J = 7.9, ArH), 7.38 (2H, d, J = 8.5, at C-3, C-5 position of Ar-C=O), 7.77 (1H, d, J = 8.8, ArH of R), 7.77 (1H, d, J = 1.9, ArH), 7.79 (1H, d, J = 1.6, ArH of R).

### 3.6.8 Compound (5h) : (E) -3-(3-(4-bromophenyl) amino) phenyl) -1-(4-(piperidin-4-ylamino) phenyl) prop-2-en-1-one

<sup>1</sup>H NMR in CDCl<sub>3</sub> (400 MHz): δ 1.53-1.79 (4H, m, 1.73 (d, J = 13.1, -H of piperidine ring), 2.39- 3.09 (4H, m, J = 9.3, -H of piperidine ring), 3.71 (1H, t, J = 10.2, -H of piperidine ring), 6.76 (1H, d, J = 15.7, =CH-CO), 6.95 (2H, d, J = 8.5, at C-2, C-6 position of ArH), 7.21 (2H, d, J = 8.9, at C-2, C-6 position of ArH of R), 7.35 (2H, d, J = 8.9, at C-3, C-5 position of ArH of), 7.36,7.49 (2H, d, J = 7.9, ArH), 7.39 (1H, d, J = 7.9, ArH), 7.53 (1H, d, J = 15.7, Ar-CH=), 7.58 (1H, t, J = 1.9, ArH), 7.68 (2H, d, J = 8.5, 1.8, at C-3, C-5 position of Ar-C=O).

## 4 Conclusion

In this research study, synthesis, characterization, and anti-microbial activity have been done on a series of piperidine-4-one derivatives. The Antimicrobial activity done with Gram-positive (*Bacillus subtilis* and *Staphylococcus aureus*) and two Gram-negative (*Escherichia coli* and *Pseudomonas aeruginosa*) bacterial strains of synthesized compounds was compared to that of standard drug and found to have good activity. Among all the compound, 5b and 5e show maximum anti-microbial activity with MIC value 6 (μg/ml) particularly against *B. subtilis* compared to Streptomycin standard drug. Which is also confirmed by molecular docking. Molecular docking is performed by Auto Dock Vina 1.2.0., 5b and 5e showed maximum Docking affinities -10.1 and -10.0 respectively against 1T2P. The SAR study showed that the electro-negative group at the R position of the phenyl ring was important for better inhibitory action. The geometry optimization in the gas phase at the B3LYP/6-31G(d,p) level of theory as implemented in Gauss5an09 DFT study. The negative values of EHOMO and ELUMO calculations for all derivatives indicate their stability which favors the chemical reactivity. Also, the ADME predictions for each derivatized molecule favors for the highest binding affinity. Additional electronic properties, such as electronegativity ( $\chi$ ), global hardness ( $\eta$ ), global softness ( $\sigma$ ), and global electrophilicity index ( $\omega$ ), were computed to ascertain the biological activity of the derivative. So, it is concluded that 5band 5e may therefore serve as lead compounds for the creation of effective antibacterial medicines.

## Acknowledgement

The authors specially thank Principal Dr. (Prof.) Keyur Shah of Shri M. M. Patel Institute of Sciences and Research, Department of Chemistry (KSV), Gandhinagar, for providing research facilities.

## References

- Rishikesan R, Karuvalam RP, Muthipeedika NJ, Sajith AM, Eeda KR, Pakkath R, et al. Synthesis of some novel piperidine fused 5-thioxo-1H-1,2,4-triazoles as potential antimicrobial and antitubercular agents. *Journal of Chemical Sciences*. 2021;133(1). Available from: <https://doi.org/10.1007/s12039-020-01872-4>.
- Zabiulla AO, H F, Am S, Al-Ghorbani M, Khanum SA. Recent investigation on heterocycles with one nitrogen [piperidine, pyridine and quinoline]. *Journal of the Iranian Chemical Society*. 2022;19(1):23–27. Available from: <https://doi.org/10.1007/s13738-021-02293-x>.
- Ramalingam A, Mustafa N, Chng WJ, Medimagh M, Sambandam S, Issaoui N. 3-Chloro-3-methyl-2,6-diarylpiperidin-4-ones as Anti-Cancer Agents: Synthesis, Biological Evaluation, Molecular Docking, and In Silico ADMET Prediction. *Biomolecules*. 2022;12(8):1093. Available from: <https://doi.org/10.3390/biom12081093>.
- Saadon KE, Taha NMH, Mahmoud NA, Elhagali GAM, Ragab A. Synthesis, characterization, and in vitro antibacterial activity of some new pyridinone and pyrazole derivatives with some in silico ADME and molecular modeling study. *Journal of the Iranian Chemical Society*. 2022;19(9):3899–3917. Available from: <https://doi.org/10.1007/s13738-022-02575-y>.
- Zala AR, Rajani DP, Kumari P. Design, synthesis, molecular docking and in silico ADMET investigations of novel piperidine-bearing cinnamic acid hybrids as potent antimicrobial agents. *Journal of the Iranian Chemical Society*. 2023;20(8):1843–1856. Available from: <https://doi.org/10.1007/s13738-023-02801-1>.
- Chen QS, Li JQ, Zhang QW. Application of Chiral Piperidine Scaffolds in Drug Design. *Pharmaceutical Fronts*. 2023;05(01):e1–e14. Available from: <https://www.thieme-connect.com/products/ejournals/pdf/10.1055/s-0043-1764218.pdf>.
- Yildiz M, Yildirim H, Bayrak N, Çakmak SM, Mataracı-Kara E, Özbek-Çelik B, et al. Design, synthesis, in vitro and in silico characterization of plastoquinone analogs containing piperidine moiety as antimicrobial agents. *Journal of Molecular Structure*. 2023;1277:134845. Available from: <https://doi.org/10.1016/j.molstruc.2022.134845>.
- Mekky AEM, Taha NAS, Mohammed NG, Hussein FRM, Abdelfattah EH, Eldin AAG, et al. Development of pyrazolo[1,5-a]pyrimidine-based antibacterial agents. *Synthetic Communications*. 2023;53(13):1053–1068. Available from: <https://doi.org/10.1080/00397911.2023.2209815>.
- Hussein AA, Slaihim MM. Synthesis, And Characterization of Some New Schiff Bases Derivatives for Piperidine, 3-Amino-1,2,4-Triazole-5-Thiolate Salt and Biological Evaluation as Antibacterial Agents. *Journal of Population Therapeutics and Clinical Pharmacology*. 2022;29(2):193–202. Available from: <https://doi.org/10.47750/jptcp.2022.971>.
- Nikonov G, Bobrov S. Comprehensive Heterocyclic Chemistry III. .
- Marinescu M. Synthesis of Antimicrobial Benzimidazole–Pyrazole Compounds and Their Biological Activities. *Antibiotics*. 2021;10(8):1002. Available from: <https://doi.org/10.3390/antibiotics10081002>.
- Shaikh TM, Debebe H. Synthesis and Evaluation of Antimicrobial Activities of Novel N-Substituted Indole Derivatives. *Journal of Chemistry*. 2020;2020:1–9. Available from: <https://doi.org/10.1155/2020/4358453>.
- Boyanova L, Gergova G, Nikolov R, Derejian S, Lazarova E, Katsarov N, et al. Activity of Bulgarian propolis against 94 Helicobacter pylori strains in vitro by agar-well diffusion, agar dilution and disc diffusion methods. *Journal of Medical Microbiology*. 2005;54(5):481–483. Available from: <https://doi.org/10.1099/jmm.0.45880-0>.
- Dan Z, Rain N, Badrul A, Adlin AR, Norazah A, A. In vitro screening of five local medicinal plants for antibacterial activity using disc diffusion method. *Tropical Biomedicine*;22(2):165–170. Available from: [https://www.msptm.org/files/165\\_-\\_170\\_In\\_vitro\\_screening.pdf](https://www.msptm.org/files/165_-_170_In_vitro_screening.pdf).
- Nielsen AB, Holder A. 2009.
- Frisch MJ, Trucks GW, Schlegel HS, Scuseria GE, Robb MA, Cheeseman JR, et al. Wallingford CT. 2013.
- Zong Y, Bice TW, Ton-That H, Schneewind O, Narayana SVL. Crystal Structures of Staphylococcus aureus Sortase A and Its Substrate Complex. *Journal of Biological Chemistry*. 2004;279(30):31383–31389. Available from: <https://doi.org/10.1074/jbc.M401374200>.
- Heaslet H, Harris M, Fahnoe K, Sarver R, Putz H, Chang J, et al. Structural comparison of chromosomal and exogenous dihydrofolate reductase from Staphylococcus aureus in complex with the potent inhibitor trimethoprim. *Proteins: Structure, Function, and Bioinformatics*. 2009;76(3):706–717. Available from: <https://doi.org/10.1002/prot.22383>.
- Zhu W, Zhang Y, Sinko W, Hensler ME, Olson J, Molohon KJ, et al. Antibacterial drug leads targeting isoprenoid biosynthesis. *Proceedings of the National Academy of Sciences*. 2013;110(1):123–128. Available from: <https://doi.org/10.1073/pnas.1219899110>.
- Narramore S, Stevenson CEM, Maxwell A, Lawson DM, Fishwick CWG. New insights into the binding mode of pyridine-3-carboxamide inhibitors of E. coli DNA gyrase. *Bioorganic & medicinal chemistry*. 2019;27:3546–3550. Available from: <https://doi.org/10.1016/j.bmc.2019.06.011>.
- Sanner MF. Python: A Programming Language for Software Integration and Development. *Journal of Molecular Graphics and Modelling*. 1999;17(1):5–7. Available from: <https://pubmed.ncbi.nlm.nih.gov/10660911/>.
- Eberhardt J, Santos-Martins D, Tillack AF, Forli S. AutoDock Vina 1.2.0: New Docking Methods, Expanded Force Field, and Python Bindings. *Journal of Chemical Information and Modeling*. 2021;61(8):3891–3898. Available from: <https://doi.org/10.1021/acs.jcim.1c00203>.
- Laskowski RA, Swindells MB. LigPlot+: multiple ligand-protein interaction diagrams for drug discovery. *Journal of Chemical Information and Modeling*. 2011;5(10):1–1. Available from: <https://doi.org/10.1021/ci200227u>.
- Daina A, Michielin O, Zoete V. SwissADME: a free web tool to evaluate pharmacokinetics, drug-likeness and medicinal chemistry friendliness of small molecules. *Scientific Reports*. 2017;7(1). Available from: <https://doi.org/10.1038/srep42717>.